Biophysical Chemistry 141 (2009) 140–152

Contents lists available at ScienceDirect

Biophysical Chemistry

journal homepage: http://www.elsevier.com/locate/biophyschem

Stress-sensitive nutrient consumption via steady and non-reversing dynamic shear in continuous-flow rotational bioreactors☆

Laurence A. Belfiore [a,b,*], Walter Bonani [b,c], Matteo Leoni [b], Carol J. Belfiore [a]

[a] Department of Chemical & Biological Engineering, Colorado State University, Fort Collins, Colorado 80523, USA
[b] Department of Materials Engineering & Industrial Technologies, University of Trento, via Mesiano 77, 38050 Trento, Italy
[c] Department of Mechanical Engineering University of Colorado, Boulder, Colorado USA 80309

ARTICLE INFO

Article history:
Received 21 September 2008
Received in revised form 8 January 2009
Accepted 8 January 2009
Available online 16 January 2009

Keywords:
Convective diffusion
Bioreactor
Stress-dependent reaction
Rotational viscometer
Stress-sensitive Damköhler number
Mammalian cell proliferation
Irreversible thermodynamics
Curie's theorem

ABSTRACT

Stress-sensitive biological response is simulated in a modified parallel-disk viscometer that implements steady and unidirectional dynamic shear under physiological conditions. Anchorage-dependent mammalian cells adhere to a protein coating on the surface of the rotating plate, receiving nutrients and oxygen from an aqueous medium that flows radially and tangentially, accompanied by transverse diffusion in the z-direction toward the active surface. This process is modeled as radial convection and axial diffusion with angular symmetry in cylindrical coordinates. The reaction/diffusion boundary condition on the surface of the rotating plate includes position-dependent stress-sensitive nutrient consumption via the zr- and $z\Theta$-elements of the velocity gradient tensor at the cell/aqueous-medium interface. Linear transport laws in chemically reactive systems that obey Curie's theorem predict the existence of cross-phenomena between scalar reaction rates and the magnitude of the second-rank velocity gradient tensor, selecting only those elements of ∇v experienced by anchorage-dependent cells that are bound to protein-active sites. Stress sensitivity via the formalism of irreversible thermodynamics introduces a zeroth-order contribution to heterogeneous reaction rates that must be quenched when nutrients, oxygen, chemically anchored cells, or vacant active protein sites are not present on the surface of the rotating plate. Computer simulations of nutrient consumption profiles via simple nth-order kinetics (i.e., $n=1,2$) suggest that rotational bioreactor designs should consider stress-sensitivity when the shear-rate-based Damköhler number (i.e., ratio of the stress-dependent zeroth-order rate of nutrient consumption relative to the rate of nutrient diffusion toward active cells adhered to the rotating plate) is greater than ≈25% of the stress-free Damköhler number. Rotational bioreactor simulations are presented for simple 1st-order, simple 2nd-order, and complex stress-free kinetics, where the latter includes a 4th-order rate expression that considers adsorption/desorption equilibria via the Fowler–Guggenheim modification of the Langmuir isotherm for receptor-mediated cell–protein binding, accompanied by the formation of receptor complexes. Dimensionless parameters are identified to obtain equivalent stress-free nutrient consumption in the exit streams of 2-dimensional creeping-flow rotational bioreactors and 1-dimensional laminar-flow tubular bioreactors. Modulated rotation of the active plate at physiological frequencies mimics pulsatile cardiovascular flow and demonstrates that these rotational bioreactors must operate above the critical stress-sensitive Damköhler number, identified under steady shear conditions, before dynamic shear has a distinguishable effect on bioreactor performance.

1. Introduction

Rotational shear in conventional viscometers is useful to stimulate the proliferation of anchorage-dependent cells and identify the critical angular velocity that induces cell–protein detachment. Larger cell–protein binding energies cause detachment to occur at higher angular velocities of the rotating plate and at radial positions that are farther from the rotation axis. These characteristics of steady-shear rotational viscometers are incorporated into a unique two-dimensional creeping-flow bioreactor to quantify the effects of viscous shear on rates of chemical reaction in stress-sensitive systems, such as anchorage-dependent cells attached to a protein layer on the surface of the rotating plate. Continuous flow of nutrients radially outward from the rotation axis is employed to avoid problems associated with a discontinuous nutrient environment when batch systems are regenerated with fresh feed at regular intervals. Assistance from non-

☆ This manuscript recognizes the life of Prof. Naz Karim's sister, Rashida Muhiuddin, who dedicated her time on this planet to serve and represent millions of people in Muktagacha, Bangladesh. She died suddenly in May 2008. Furthermore, this manuscript commemorates the 100th anniversary of the birth of Alphonse Vincent Belfiore on May 8th, 1909.

* Corresponding author. Department of Chemical & Biological Engineering, Colorado State University, Fort Collins, Colorado 80523, USA.
E-mail address: belfiore@engr.colostate.edu (L.A. Belfiore).

0301-4622/$ – see front matter © 2009 Elsevier B.V. All rights reserved.
doi:10.1016/j.bpc.2009.01.003

equilibrium thermodynamics provides a fundamental approach to describe stress-dependent nutrient consumption at the cell/aqueous-medium interface. Under isotropic conditions where the transport coefficients are scalars, flux-*i* is coupled to force-*j* if the tensorial ranks of flux-*i* and force-*j* are the same or if they differ by an even integer [1–3]. This classic theorem for flux-force relations is known as the Curie restriction in isotropic systems, proposed by P. Curie in 1903 [1]. As a consequence of Curie's theorem in N-component systems, via the transport-phenomena-based rate of entropy production per volume of fluid, there are N first-rank tensorial fluxes that are coupled to N first-rank tensorial forces via linear laws [3]. Soret diffusion and Dufour conduction represent examples of these couplings between vector fluxes and driving forces in heat and mass transfer [4,5]. Curie's theorem predicts that scalar rates of production of the mass of species *i* due to chemical reaction should be coupled to a scalar representation of the velocity gradient tensor, in addition to any convective enhancement resulting from a reduction in the mass transfer boundary layer thickness adjacent to the active surface. This formalism is employed to construct heterogeneous rates of nutrient consumption and mammalian cell proliferation that are stimulated by viscous shear [6]. There are practical examples where tensile stress stimulates the response of smooth muscle cells [7], compressive stress stimulates nutrient consumption by bone cells [8,9], and shear accelerates the proliferation of endothelial cells [6]. Hence, one constructs the *magnitude of the velocity gradient tensor*, not its *trace* or determinant, to quantify *shear*-stress-sensitive rates of nutrient consumption by selecting only those elements of ∇v that act across the surface of the rotating plate where anchorage-dependent cells bind to proteins. This methodology introduces a zeroth-order contribution to heterogeneous reaction rates that must be quenched via *Heaviside step functions* when nutrients, oxygen, chemically anchored cells, or vacant active protein sites are not present on the surface of the rotating plate. The primary motivation for this investigation includes (i) the use of conventional rotating-disk viscometers that exhibit position-dependent viscous shear at the active surface where anchorage-dependent cells consume nutrients, (ii) comparisons between steady shear in geometrically dissimilar tubular and rotational bioreactors, and (iii) implementation of dynamic shear in the rotating-disk geometry via angular velocity modulations at physiological frequencies to simulate pulsatile cardiovascular flow.

2. Stress-sensitive rotational bioreactor model

2.1. Schematic representation of the rotational bioreactor

The conditions in this creeping-flow parallel-disk configuration combine two classic problems from Newtonian fluid dynamics, as illustrated in Fig. 1. Solid-body rotation of the upper plate at $z=2B$ induces either steady (i.e., $A=0$) or dynamic (i.e., $A=\Omega$) tangential fluid motion. The introduction of fresh nutrient feed that enters the bioreactor through the center of the rotating shaft at $r=R_{\text{inlet}}$ is responsible for flow radially outward. Nutrient depletion in the exit stream at the outer edge of both plates (i.e., $r=R_{\text{Plate}}$) is predicted via integration of the microscopic nutrient mass density profile with respect to Θ (i.e., $0\le\Theta\le2\pi$) and z (i.e., $0\le z\le2B$).

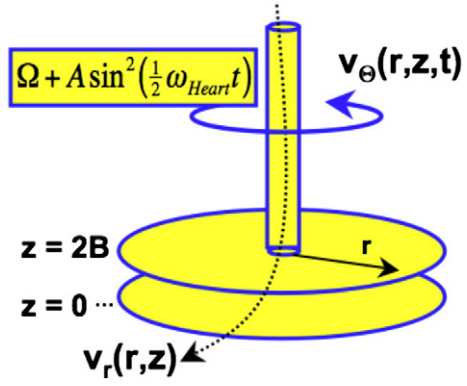

Fig. 1. Schematic illustration of the parallel-disk bioreactor with 2-dimensional creeping flow and non-reversing dynamic shear at the surface of the rotating plate, where cells are seeded at $z=2B$. Steady shear is obtained when the peak-to-peak amplitude A of angular velocity modulations vanishes. The lower plate at $z=0$ is stationary and inert.

2.2. Receptor-mediated cell–protein binding

Active poly(amino acid) sites are identified by favourable protein conformations within an aqueous layer on the surface of the rotating plate (i.e., $z=2B$) that expose functional groups which participate in interactions with cell receptors. Attachment of cell receptors to these protein sites is described by the Fowler–Guggenheim modification of the Sipps isotherm [10–12];

$$\Theta_{\text{Cell}} = 1-\Theta_{\text{Vacant}} = \frac{\left\{K_{\text{Cell}}(T)[\rho_{\text{Cell}}]_{z=2B}\exp(-\varphi\Theta_{\text{Cell}})\right\}^{1/\lambda}}{1+\left\{K_{\text{Cell}}(T)[\rho_{\text{Cell}}]_{z=2B}\exp(-\varphi\Theta_{\text{Cell}})\right\}^{1/\lambda}} \quad (1)$$

where Θ_{Cell} represents the fraction of active sites occupied by cells, Θ_{Vacant} is the vacant site fraction, ρ_{Cell} is the local cell surface density (i.e., mass of free and bound cells per unit area of protein-coated surface), and K_{Cell} is the temperature-dependent adsorption–desorption (i.e., association) equilibrium constant with dimensions of length squared per mass. The statistical thermodynamic derivation [11,12] of Eq. (1) accounts for interactions between adsorbed cells on adjacent active sites via the formation of receptor complexes. The cell–cell interaction energy Ξ is negative to simulate chemical bonding, and $\varphi=\Xi/(k_{\text{Boltzmann}}T)$. Cell–cell attraction and the formation of chemical bonds between receptors (i.e., $\Xi<0$, $\varphi<0$) increases Θ_{Cell} at the same cell mass density [13]. Hence, stronger chemical bonds between adjacent receptors, due to the formation of receptor complexes, and stronger cell–protein binding energies increase cell fractional surface coverage. One recovers the Sipps isotherm from Eq. (1) when the interaction energy between receptor complexes on adjacent active sites vanishes (i.e., $\varphi=0$). The Sipps exponent (i.e., $1/\lambda$) on cell mass density in Eq. (1) corresponds to the Hill coefficient. The Hill equation for protein–ligand binding [14], which is mathematically similar to the Sipps isotherm in heterogeneous catalysis, describes the equilibrium fraction of active protein sites occupied by ligands (i.e., cell receptors). One recovers the Langmuir isotherm when the Hill coefficient λ^{-1} is unity for non-cooperative binding. Hill coefficients greater than unity (i.e., $0<\lambda<1$) correspond to cooperative protein–cell binding, where protein conformational changes occur after the first cell receptor docks to permit subsequent docking with greater affinity.

2.3. Stress-free rate of nutrient consumption

Within reasonable physiological limits, a 4th-order *stress-free* heterogeneous reaction rate for nutrient consumption is expressed in terms of (i) nutrient and oxygen mass densities near the surface of the rotating plate at $z=2B$, (ii) surface coverage fraction of cells on active sites, Θ_{Cell}, which is related to cell mass density via Eq. (1), and (iii) vacant site fraction, Θ_{Vacant}, which is required for cells to consume nutrients aerobically and increase their mass density via chemisorption as a monolayer on the protein-active surface. Hence, the complex *stress-free* rate of nutrient consumption, with dimensions of nutrient mass per surface area per time, is;

$$-R_{A,\text{SurfaceRx}} = k_{\text{Surface}}\{\rho_{\text{Nutrient}}\}_{z=2B}\{\rho_{\text{Oxygen}}\}_{z=2B}\Theta_{\text{Cell}}\Theta_{\text{Vacant}} \quad (2)$$
$$\Theta_{\text{Cell}}+\Theta_{\text{Vacant}}=1$$

Eq. (2) provides a mathematical representation of the rate of nutrient consumption at the cell/aqueous-medium interface (i.e., $z=2B$). The analog in heterogeneous catalysis is a dual-site chemical-reaction rate-controlling mechanism in which nutrients and dissolved oxygen from the aqueous medium are consumed by protein-bound cells such that nutrients and oxygen do not occupy active protein sites on the surface of the rotating plate [3].

2.4. Stoichiometric requirements via bulk and surface diffusion

Surface diffusion [15] is invoked to describe cell mobility within the aqueous protein layer that coats the rotating plate, where cell receptor diffusivities range from 10^{-9}–10^{-10} cm^2/s [16]. This phenomenon is required to develop relations between nutrient mass density at the cell/aqueous-medium interface and cell mass density on protein-coated surfaces. One invokes a balance between diffusion and reaction at the rotating plate in the parallel-disk configuration. Nutrients diffuse in the positive z-direction toward anchorage-dependent cells, as specified by the rate of nutrient consumption. At steady state, this nutrient balance is connected to the rate of cell proliferation, followed by surface diffusion of newly produced biomass away from the site of nutrient consumption. Surface diffusion is not a mechanism of cell motility, but it provides a phenomenological description of cell movement that is sufficiently general to include a variety of locomotive mechanisms where cells respond to stimuli by altering their velocity via stochastic fluctuations [17]. If angular symmetry is a reasonable assumption, such that cell mass density in the aqueous protein coating on the rotating plate is independent of the polar angle in cylindrical coordinates, then the desired relation between nutrient diffusion in the z-direction, within the mass transfer boundary layer, and surface diffusion of adhered cells radially outward on the surface is given by;

$$-\frac{1}{\varepsilon_{\text{Nutrient}}}D_{\text{Nutrient}}\left\{\frac{\partial\rho_{\text{Nutrient}}}{\partial z}\right\}_{z=2B}=\frac{1}{2B}\frac{D_{\text{Cell}}}{\varepsilon_{\text{Cell}}}\left\{\frac{d\rho_{\text{Cell}}}{dr}\right\} \tag{3}$$

where $\varepsilon_{\text{Cell}}/\varepsilon_{\text{Nutrient}}$ (i.e., ≈25%) represents the ratio of cell mass produced relative to nutrient mass depleted during nutrient consumption and cell proliferation, during nutrient consumption and cell proliferation, because some nutrient consumption is channeled into other products and metabolic activities not related to cell proliferation, such as energetic support for cell motility in the protein-coated layer on the rotating surface. Viscous shear stresses cell motility in the protein-coated layer on the rotating surface. Viscous shear stresses τ_{zr} and $\tau_{z\Theta}$ at the cell/aqueous-medium interface (i.e., $z=2B$) influence cell motility along the surface. The appropriate use of cell surface density ρ_{Cell} in Fick's first law on the right side of Eq. (3) requires an additional factor [i.e., the active-surface-area-to-volume ratio = 1/(2B)] because surface diffusional mass flux that incorporates ρ_{Cell} in Fick's law yields dimensions of mass per *length*-time. Analogous to Eq. (3), there exists a relation between nutrient and oxygen diffusional mass fluxes in the z-direction, evaluated near the active surface, according to the cascade of physiological reactions that occur;

$$\frac{1}{\varepsilon_{\text{Nutrient}}}D_{\text{Nutrient}}\left\{\frac{\partial\rho_{\text{Nutrient}}}{\partial z}\right\}_{z=2B}=\frac{1}{\varepsilon_{\text{Oxygen}}}D_{\text{Oxygen}}\left\{\frac{\partial\rho_{\text{Oxygen}}}{\partial z}\right\}_{z=2B} \tag{4}$$

Each side of Eq. (4), with dimensions of mass per area-time, depends on radial position r at the surface of the rotating plate. Hence, integration from the inlet where fresh nutrient feed enters the configuration at $r=R_{\text{inlet}}$ to any radial position r further from the rotation axis (i.e., $R_{\text{inlet}}\le r\le R_{\text{Plate}}$) provides an approximation for the mass density of oxygen near the active surface, which is required for quantitative evaluation of the rate of nutrient consumption. Ordinary molecular diffusion coefficients for nutrients and oxygen in the aqueous medium scale inversely with the square-root of molecular weight [18], $\varepsilon_{\text{Oxygen}}/\varepsilon_{\text{Nutrient}}$ (i.e., ≈4%) represents the ratio of oxygen mass depleted relative to nutrient mass depleted during nutrient consumption, and within reasonable physiological limits, the inlet mass density of dissolved oxygen is approximately 5–7% of the inlet nutrient mass density. If the stoichiometry of oxygen-to-nutrient consumption is affected when anchorage-dependent cells are subjected to viscous shear, then the initial condition should consider this modification to guarantee that a sufficient amount of oxygen is available for aerobic nutrient consumption.

2.5. Mathematically correct form of the coupling between scalar reaction rates and the asymmetric velocity gradient tensor

It is necessary to address the correct quantitative construction of nutrient consumption rates that are affected by viscous shear at the cell/aqueous-medium interface. Mathematical inconsistencies must be avoided if scalars and second-rank tensors are coupled via scalar coupling coefficients, as required for isotropic systems. Hence, one should employ a scalar *invariant* of the velocity gradient tensor in the rate of nutrient consumption because these invariants of ∇v are independent of the choice of the coordinate system used to express this tensor [18]. If ∇v is denoted by g, and 2 other tensors are defined by $g^2=g\cdot g$ and $g^3=g\cdot\{g\cdot g\}=g\cdot g^2$, then three independent scalar invariants of the velocity gradient tensor are constructed by taking the trace of g, g^2, and g^3 [18]. Shear elements are not included in *Trace{g}*, which is equivalent to $\nabla\cdot v=0$ for incompressible flow. $Trace\{g^2\}=2g_{12}g_{21}=2[\nabla v]_{r\Theta}[\nabla v]_{\Theta r}=-2\Omega^2$ is the only nonzero scalar invariant in this rotational bioreactor with creeping flow in two coordinate directions and four non-zero elements of the velocity gradient tensor on the surface of the rotating plate. Unfortunately, $Trace\{g^2\}=-2\Omega^2$ contains no information about *position-dependent shear* that is embedded in g_{31} and g_{32} {i.e., $[\nabla v]_{zr}$ and $[\nabla v]_{z\Theta}$ via Eq. (6)}, as discussed in the next section. Another possibility is to construct the *magnitude of the velocity gradient tensor*, defined by the square-root of the double-dot product of the velocity gradient tensor with the transpose of the velocity gradient tensor [18];

$$\text{Magnitude of the velocity gradient tensor; } |\nabla v|=\sqrt{\frac{1}{2}\{\nabla v\}:\{\nabla v\}^T}=\sqrt{\frac{1}{2}\sum_{i,j}g_{ij}^2} \tag{5}$$

The factor of 0.5 under the square-root in Eq. (5) guarantees that the magnitude of a symmetric 2nd-rank tensor reduces to its only independent off-diagonal element when all other elements vanish. However, one must recognize that ∇v is not a symmetric 2nd-rank tensor.

2.6. Magnitude of the position-dependent velocity gradient tensor on the surface of the rotating plate for 2-dimensional creeping flow

This bioreactor exhibits 2-dimensional creeping flow of a Newtonian culture medium in the r- and Θ-directions [i.e., $v_r(r,z)$ and $v_\Theta(r,z)$], and six non-zero elements of the velocity gradient tensor (i.e., rr, $r\Theta$, Θr, $\Theta\Theta$, zr, and $z\Theta$ elements of ∇v), in general [18]. Some of these scalar elements of ∇v vanish at the surface of the rotating plate (i.e., rr and $\Theta\Theta$ elements of ∇v vanish at $z=2B$), and two other shear elements of ∇v do not act across the flat surface at $z=2B$ where cell receptors bind to active protein sites (i.e., $r\Theta$ and Θr elements describe shear across surfaces at constant r and constant Θ, respectively). The following analysis provides a reasonable estimate of the "shear rate" at $z=2B$. If the "no-slip" condition is obeyed at the cell/aqueous-medium interface, then an analysis of solid-body rotation at $z=2B$ suggests that $v_\Theta(r,z)=rf(z)$, whereas the Equation of Continuity reveals that $v_r(r,z)=c(z)/r$.

The no-slip condition is used to calculate shear stress at the rotating plate, and this is independent of how cells respond mechanically to shear. If cells remain anchored to active protein sites, then there should be no conflict between the no-slip condition and elastic cell response in the presence of shear under creeping flow conditions [19]. One solves the r- and Θ-components of the Equation of Motion independently to obtain expressions for $c(z)$ and $f(z)$, respectively. *Decoupled* velocity profiles for incompressible Newtonian fluids at low Reynolds numbers [18] simultaneously satisfy the r- and Θ-components of the Equation of Motion when forces due to convective momentum flux are negligible and dependence on the polar angle is neglected via angular symmetry. Four nonzero elements of the velocity gradient tensor, evaluated at $z=2B$ in cylindrical coordinates, are summarized in Eq. (6) when the upper plate rotates at angular velocity Ω and the culture medium flows radially outward between the plates with volumetric flowrate $Q_{\text{Volumetric}}$;

$$v_\Theta(r,z)=\Omega r\left\{\frac{z}{2B}\right\}$$
$$v_r(r,z)=\frac{3Q_{\text{Volumetric}}}{8\pi B^2}\frac{z}{r}\left\{2-\frac{z}{B}\right\}$$
$$\{[\nabla v]_{r\Theta}\}_{z=2B}=\left\{\frac{\partial v_\Theta}{\partial r}\right\}_{z=2B}=\Omega;\ \{[\nabla v]_{\Theta r}\}_{z=2B}=\left\{\frac{1}{r}\frac{\partial v_r}{\partial\Theta}-\frac{v_\Theta}{r}\right\}_{z=2B}=-\Omega;$$
$$\{[\nabla v]_{z\Theta}\}_{z=2B}=\left\{\frac{\partial v_\Theta}{\partial z}\right\}_{z=2B}=\frac{\Omega r}{2B};\ \{[\nabla v]_{zr}\}_{z=2B}=\left\{\frac{\partial v_r}{\partial z}\right\}_{z=2B}=-\frac{3Q_{\text{Volumetric}}}{4\pi B^2 r}. \tag{6}$$

When homogeneous chemical reactions occur *volumetrically* throughout the culture medium, all nonzero scalar elements of ∇v contribute to stress-sensitive nutrient consumption. However, cell receptors bind to active protein sites and the consumption of nutrients is a *surface-related process*. Consequently, it is only necessary to consider the $z\Theta$- and zr-elements of ∇v that are operative across this active surface (i.e., when the first subscript on ∇v is z). The *magnitude of the velocity gradient tensor* on the surface of the rotating plate is modified in Eq. (7) to reflect this fundamental difference between the effects of viscous shear on homogeneous volumetric reactions vs. heterogeneous surface reactions;

$$|\nabla v(r)|_{z=2B}=\sqrt{\frac{1}{2}\{\nabla v\}:\{\nabla v\}^T}$$
$$=\sqrt{\frac{1}{2}\sum_{i,j}g_{ij}^2}\ \overset{\substack{\text{select nonzero}\\ \text{scalar elements}\\ \Rightarrow\\ \text{that act across}\\ \text{the surface at } z=2B}}{}\ \sqrt{\frac{1}{2}\left[\left\{\frac{\Omega r}{2B}\right\}^2+\left\{\frac{3Q_{\text{Volumetric}}}{4\pi B^2 r}\right\}^2\right]} \tag{7}$$

2.7. Linear law for stress-dependent rates of nutrient consumption

If one focuses on fluxes and driving forces that appear as products in the rate of entropy generation per unit volume s_G for binary mixtures, from the transport-phenomena-based equation of change for fluid entropy [3];

$$s_G=\left\{\begin{array}{l}-\left(q_{\text{Conduction}}-\left[\frac{\mu_{\text{A,ChemPotential}}}{MW_A}-\frac{\mu_{\text{B,ChemPotential}}}{MW_B}\right]j_{\text{A,Diffusion}}\right)\cdot\frac{1}{T^2}\nabla T\\ -j_{\text{A,Diffusion}}\cdot\frac{1}{T}\left\{\left(g_{\text{B,ForceField}}-g_{\text{A,ForceField}}\right)+\nabla\left[\frac{\mu_{\text{A,ChemPotential}}}{MW_A}-\frac{\mu_{\text{B,ChemPotential}}}{MW_B}\right]\right\}\\ -R_{A,\text{SurfaceRx}}\frac{1}{T}\left[\frac{\mu_{\text{A,ChemPotential}}}{MW_A}-\frac{\mu_{\text{B,ChemPotential}}}{MW_B}\right]\\ -\tau_{\text{ViscousStress}}:\frac{1}{T}\{\nabla v\}_{\text{VelocityGradientTensor}}\end{array}\right\} \tag{8}$$

then Curie's theorem suggests that the scalar flux $-R_{A,\text{SurfaceRx}}$, better known as the rate of nutrient consumption, with dimensions of nutrient mass per surface area per time, should depend linearly on both scalar and 2nd-rank tensor driving forces that appear on the right sides of the 3rd and 4th lines of s_G. If necessary, $R_{A,\text{SurfaceRx}}$ can be written in pseudo-volumetric form via multiplication by the active-surface-to-volume ratio of the bioreactor, $=1/\{2B\}$. For pseudo-binary systems that are not far removed from *equilibrium*, the appropriate *linear law* that satisfies Curie's restriction is written in the following form;

Generalized kinetic rate law for stress−sensitive nutrient consumption on active surfaces

$$-R_{A,\text{SurfaceRx}}=\xi_{A1}\frac{1}{T}\left\{\frac{\mu_A}{MW_A}-\frac{\mu_B}{MW_B}\right\}+\xi_{A2}\frac{1}{T}\sqrt{\frac{1}{2}\{\nabla v\}:\{\nabla v\}^T}$$

Onsagercoupling coefficients; ξ_{A1} and ξ_{A2}

$$\xi_{A1}=\alpha T;\ \xi_{A2}=\gamma T$$

Nonlinear effects are included in the stress−free rate of nutrient consumption

$$-R_{A,\text{SurfaceRx}}=k_{\text{Surface}}\{\rho_{\text{Nutrient}}\}_{z=2B}\{\rho_{\text{Oxygen}}\}_{z=2B}\Theta_{\text{Cell}}\Theta_{\text{Vacant}}+\gamma\sqrt{\frac{1}{2}\sum_{i,j}g_{ij}^2}$$
$$g_{ij}=\{\nabla v\}_{ij-\text{element in the }3\times3\text{ velocity gradient matrix evaluated at }z=2B} \tag{9}$$

Nonlinearity has been introduced in the reaction rate expression by focusing on the diagonal contribution due to *stress-free* chemical kinetics, not the contribution from viscous stress at low shear rates in the creeping flow regime. Hence, the diagonal (i.e., scalar) contribution to the previous kinetic rate expression [i.e., Eq. (9)], based on differences between chemical potentials (i.e., *the affinity*), has been modified via Eq. (2) which corresponds to a complex 4th-order stress-free nonlinear rate law for biochemical reactions. The linear cross-term should be appropriate under low-shear conditions that are characteristic of creeping flow. The form of Eq. (9) is sufficiently flexible to account for viscous shear at the active surface that might change the reaction pathway or the products of nutrient consumption if another parallel pathway were equally important, relative to the stress-free kinetic contribution. Furthermore, the stoichiometry of nutrient consumption (i.e., mass of oxygen consumed per mass of nutrients consumed, $\varepsilon_{\text{Oxygen}}/\varepsilon_{\text{Nutrient}}$, and mass of cells generated per mass of nutrients consumed, $\varepsilon_{\text{Cell}}/\varepsilon_{\text{Nutrient}}$) might be different for stress-dependent rates of nutrient consumption relative to the stress-free consumption rates. Zeroth-order mechano-sensitive rates of nutrient consumption do not require stoichiometry to quantify the kinetic rate expression, but the initial condition should be modified to guarantee that a sufficient amount of oxygen is available for aerobic nutrient consumption.

2.8. Mass transfer equation

Bioreactor performance is established by calculating the mass density of nutrients from Eq. (10) that accounts for radial convection and transverse diffusion at steady state. Nutrient consumption appears in the boundary condition at $z=2B$. Ideal bioreactor analysis at large mass transfer Peclet numbers in cylindrical coordinates, with negligible radial diffusion compared to radial convection, is described by;

$$v_r(r,z)\frac{\partial\rho_{\text{Nutrient}}}{\partial r}=D_{\text{Nutrient}}\frac{\partial^2\rho_{\text{Nutrient}}}{\partial z^2} \tag{10}$$

The axisymmetric nature of this bioreactor justifies the neglect of tangential convective mass transfer of nutrients, even though $v_\Theta\neq0$. This is consistent with previous models of 3-dimensional flow in rotational bioreactors [20]. Recently, microscopic convective diffusion models of kidney transport have been developed to describe shear-stress-mediated effects of blood flow on nitric oxide consumption [21].

2.8.1. Zeroth-order stress-sensitive rate of nutrient consumption on the surface of the rotating plate

A qualitative description of the boundary conditions considers a balance between the rate of nutrient transport toward the protein-coated

surface via molecular mass transfer and the rate of nutrient consumption that contains stress-free and stress-dependent contributions. The mathematical expression for this balance at $z=2B$ is;

$$-D_{\text{Nutrient}}\left\{\frac{\partial \rho_{Nutrient}}{\partial z}\right\}_{z=2B} = k_{\text{cell,Surface}}\{\rho_{Nutrient}\}_{z=2B}\{\rho_{\text{Oxygen}}\}_{z=2B}\Theta_{\text{Cell}}\Theta_{\text{Vacant}} + \gamma \text{H}\{\rho_{\text{Nutrient}}(\text{r},\text{z}=2\text{B})\}\sqrt{\frac{1}{2}\sum_{\text{i,j}} g_{\text{ij}}^2} \quad (11)$$

Both processes have dimensions of nutrient mass per area per time, and the Onsager coupling coefficient γ has dimensions of nutrient mass per area of active protein sites that exhibit the appropriate conformation for receptor-mediated cell–protein binding. The stress-dependent contribution to the rate of nutrient consumption in Eq. (11) is classified as a zeroth-order reaction because it does not exhibit *explicit* dependence on the mass density of any species. However, this term must be extinguished when nutrients are not available for immediate consumption by anchorage-dependent cells due to extreme diffusion-limited conditions in the mass transfer boundary layer near $z=2B$. *Heaviside step functions*, $H\{\rho_{\text{Nutrient}}(r,z=2B)\}$, are employed in the reaction/diffusion boundary condition to terminate the stress-dependent contribution to nutrient consumption when reaction is sufficiently faster than diffusion in the z-direction at large Damköhler numbers. Three additional factors that contain step functions are included in the dimensionless form of Eq. (11) to account for the absence of (i) cells and vacant sites on the active surface, and (ii) oxygen within the cells after a reasonable time lag when anaerobic proliferation is no longer feasible. Computations that exclude step functions in the stress-dependent contribution to nutrient consumption are vulnerable to the prediction of unrealistic negative species concentrations at the active boundary. Zero-flux is invoked on the surface of the stationary plate, which does not contain an aqueous protein coating or chemisorbed cells, so nutrient consumption does not occur at $z=0$.

2.9. Dimensionless equations for 2-dimensional creeping flow in the parallel-disk configuration with stress-sensitive rates of nutrient consumption on the surface of the rotating plate

2.9.1. Dimensionless variables and parameters for nth-order irreversible chemical kinetics

These design equations include radial convection, transverse diffusion in the z-direction, and simple nth-order rates of nutrient consumption that depend on nutrient mass density near the surface of the rotating plate. The problem description contains three important dimensionless parameters; (i) the mass transfer Peclet number, Pe_{MT} (i.e., rate of convective mass transfer divided by rate of molecular mass transfer), (ii) the ordinary Damköhler number, $\beta_{0,n\text{th-order}}$, for stress-free heterogeneous nutrient consumption (i.e., stress-free consumption rate divided by rate of molecular mass transfer), and (iii) the stress-sensitive Damköhler number β_{Stress} for viscous-shear-enhanced nutrient consumption at the cell/aqueous-medium boundary (i.e., stress-dependent consumption rate divided by the rate of nutrient diffusion toward anchorage-dependent cells). A factor of $2B$ in the dimensional scaling factor for cell mass density represents the volume-to-active-surface-area ratio of the rotational bioreactor, where the active surface describes the surface area of the rotating plate that contains bound cells. The factor of $2B$ is required because nutrient mass density is volumetric within the aqueous medium, whereas cell mass density is a surface-related concentration within the aqueous protein coating on the rotating plate. The steady angular velocity Ω of the rotating plate is a convenient experimental variable that allows one to perform systematic parametric sensitivity simulations based on the stress-sensitive Damköhler number, β_{Stress}, defined in terms of the steady-shear magnitude of the velocity gradient tensor at the outer edge of the rotating plate, with no angular velocity modulations [i.e., $A=0$]. If the thickness between the plates (i.e., $2B=$volume-to-active-surface-area ratio) is chosen as the *characteristic length* to dimensionalize the radial r and axial z spatial variables, then;

Radial independent variable; $r = 2B\eta$
Axial independent variable; $z = 2B\zeta$
Nutrient mass density; $\rho_{\text{Nutrient}} = \rho_{\text{Nutrient,Bulk}}(r = R_{\text{inlet}})\Psi_{\text{Nutrient}}$
Oxygen mass density; $\rho_{\text{Oxygen}} = \rho_{\text{Nutrient,Bulk}}(r = R_{\text{inlet}})\Psi_{\text{Oxygen}}$
Cell mass density; $\rho_{\text{Cell}} = 2B\rho_{\text{Nutrient,Bulk}}(r = R_{\text{inlet}})\Psi_{\text{Cell}}$
Mass transfer Peclet number; $Pe_{\text{MT}} = \frac{R_{\text{Plate}}\langle v_r(r=R_{\text{Plate}})\rangle}{D_{\text{Nutrient}}} = \frac{Q_{\text{Volumetric}}}{4\pi B D_{\text{Nutrient}}}$
$Q_{\text{Volumetric}} = 4\pi B R_{\text{Plate}}\langle v_r(r=R_{\text{Plate}})\rangle$
Stress−free Damkohler number (nth−order);

$$\beta_{0,n^{\text{th}}-\text{order}} = \frac{2Bk_{n,\text{Surface}}\left\{\rho_{\text{Nutrient,Bulk}}(r=R_{\text{inlet}})\right\}^{n-1}}{D_{\text{Nutrient}}}$$

Stress−dependent Damkohler number;

$$\beta_{\text{Stress}} = \frac{2B\gamma\,|\,\nabla v(r=R_{\text{Plate}})\,|_{z=2B}}{D_{\text{Nutrient}}\rho_{\text{Nutrient,Bulk}}(r=R_{\text{inlet}})} = \frac{2B\gamma}{D_{\text{Nutrient}}\rho_{\text{Nutrient,Bulk}}(r=R_{\text{inlet}})}\frac{R_{\text{Plate}}}{2B}\sqrt{\frac{1}{2}\left[\Omega^2 + \left\{\frac{3}{\tau_{\text{Residence}}}\right\}^2\right]} \quad (12)$$

2.9.2. Dimensionless mass transfer equation

In the creeping flow regime at large mass transfer Peclet numbers, the partial differential equation with variable coefficients that must be solved for dimensionless nutrient mass density is;

$$6Pe_{\text{MT}}\frac{\zeta}{\eta}(1-\zeta)\frac{\partial \Psi_{\text{Nutrient}}}{\partial \eta} = \frac{\partial^2 \Psi_{\text{Nutrient}}}{\partial \zeta^2} \quad (13)$$

The radial derivative (i.e., with respect to r, or η) is written using first-order-correct finite differences, whereas diffusion toward active protein sites on the rotating plate [i.e., 2nd-derivative with respect to z, or ζ, on the right side of Eq. (13)] is implicit at the new radial position using second-order-correct finite-difference analogs. If $2B$ is employed as the characteristic length for Pe_{MT} in Eq. (12), then an additional multiplicative factor of $R_{\text{Plate}}/2B$ must be included on the left side of Eq. (13).

2.9.3. Separability of the mass transfer equation

It is possible to identify the nature of the radial and axial functions [i.e., $F(\eta)$ and $G(\zeta)$, respectively] that represent a separation-of-variables solution to Eq. (13), prior to generating numerical results. If $\Psi_{\text{Nutrient}}(\eta,\zeta)=F(\eta)G(\zeta)$, then the dimensionless mass transfer equation reveals that;

$$\frac{\text{d}\ln F}{\text{d}\eta} = -\frac{\chi^2}{6Pe_{\text{MT}}}\eta \Rightarrow F(\eta)\approx \exp\left\{-\frac{\chi^2}{12Pe_{\text{MT}}}\eta^2\right\} \quad (14)$$

$$\frac{d^2G}{d\zeta^2} + \chi^2\zeta(1-\zeta)G(\zeta) = 0$$

where χ is real such that $-\chi^2$ is a negative *separation constant* which prevents $F(\eta)$ from increasing unrealistically in unbounded fashion at large radial positions from the center of the rotating plate. $G(\zeta)$ is given by a linear combination of *Parabolic Cylinder* functions, also known as Weber functions, that represent the solution to Weber's differential equation.

2.9.4. Dimensionless boundary conditions and magnitude of the velocity gradient tensor

Both types of Damköhler numbers appear in the reaction/diffusion boundary condition at $z=2B$, where cell receptors bind to active

protein sites. For simple *n*th-order stress-free kinetics that depend only on nutrient mass density at the cell/aqueous-medium interface, the appropriate boundary conditions are;

$$\Psi_{\text{Nutrient}} = 1 @ \eta = \eta_{\text{start}}, 0 \le \zeta < 1$$

$$\left\{\frac{\partial \Psi_{\text{Nutrient}}}{\partial \zeta}\right\}_{\zeta=0} = 0$$

$$-\left\{\frac{\partial \Psi_{\text{Nutrient}}}{\partial \zeta}\right\}_{\zeta=1} = \beta_{0,n\text{th}-\text{order}} \Psi^{n}_{\text{Nutrient}}(\eta, \zeta = 1) + H\{\Psi_{\text{Nutrient}}(\eta, \zeta = 1)\}\beta_{\text{Stress}}\Gamma(\eta)$$

$$\Gamma(\eta) = \frac{|\nabla v(r)|_{z=2B}}{|\nabla v(r=R_{\text{Plate}})|_{z=2B}} = \frac{2B}{R_{\text{Plate}}}\left[\frac{\eta^2\Omega^2 + \left\{\frac{3}{\tau_{\text{Residence}}}\left(\frac{R_{\text{Plate}}}{2B}\right)^2\right\}^2 \frac{1}{\eta^2}}{\Omega^2 + \left\{\frac{3}{\tau_{\text{Residence}}}\right\}^2}\right]^{\frac{1}{2}} \tag{15}$$

The position-dependent magnitude of the dimensionless velocity gradient tensor on the surface of the rotating plate, defined by $\Gamma(\eta)$ in Eq. (15), is illustrated in Fig. 2. The bioreactor inlet tube is designed with assistance from the graphs in Fig. 2 by selecting $R_{\text{inlet}}/2B \approx 5$ and 400 s $\le \tau_{\text{Residence}} \le$ 800 s such that anchorage-dependent cells attached to the rotating plate near R_{inlet} do not experience significantly large shear rates, partly due to entrance effect that might induce cell detachment from the surface.

All parameters employed in Fig. 2 are consistent with the creeping flow assumption, as verified in the next section. The position-dependent magnitude of the velocity gradient tensor, which appears in the stress-sensitive rate of nutrient consumption on the surface of the rotating plate, has been modified by selecting only those elements that act across the surface at $z = 2B$ [i.e., see Eq. (7)], and dimensionalized as follows;

$$\frac{|\nabla v(\eta)|_{\zeta=1}}{\Omega} = \sqrt{\frac{1}{2}\left[\eta^2 + \left\{\frac{3Q_{\text{Volumetric}}}{8\pi B^3 \Omega}\right\}^2 \frac{1}{\eta^2}\right]} \tag{16}$$

$$= \sqrt{\frac{1}{2}\left[\eta^2 + \left\{\frac{3}{\Omega\tau_{\text{Residence}}}\left(\frac{R_{\text{Plate}}}{2B}\right)^2\right\}^2 \frac{1}{\eta^2}\right]}$$

2.9.5. Verification of the creeping flow assumption

For 2-dimensional creeping flow, it seems reasonable to use the product of the characteristic length (i.e., gap thickness between the two plates, $2B$) and the magnitude of the velocity gradient tensor evaluated at the outer edge of the rotating plate, via Eq. (5) instead of Eq. (7) or (16), as an *order-of-magnitude* estimate of the fluid's average velocity in the construction of the Reynolds number, *Re*. Since there are four non-zero elements of the velocity gradient tensor on the surface of the rotating plate, given by Eq. (6), one obtains the following expression for *Re* that identifies upper limits on geometric and flow parameters to satisfy the creeping flow assumption;

$$Re = \frac{\rho}{\mu}(2B)^2 |\nabla v(r=R_{\text{Plate}})|_{z=2B} \tag{17}$$

$$= \frac{\rho}{\mu}(2B)^2 \sqrt{\frac{1}{2}\left[2\Omega^2 + \left\{\frac{\Omega R_{\text{Plate}}}{2B}\right\}^2 + \left\{\frac{3Q_{\text{Volumetric}}}{4\pi B^2 R_{\text{Plate}}}\right\}^2\right]}$$

$$= \frac{\rho}{\mu}(2B)^2 \Omega \sqrt{\frac{1}{2}\left[2 + \left\{\frac{R_{\text{Plate}}}{2B}\right\}^2 + \left\{\frac{3}{\Omega\tau_{\text{Residence}}}\left(\frac{R_{\text{Plate}}}{2B}\right)\right\}^2\right]} < 1$$

Another construction of *Re* that employs the *magnitude of the velocity vector* via the average radial velocity at $r = R_{\text{Plate}}$ and the tangential velocity at the outer edge of the rotating plate yields;

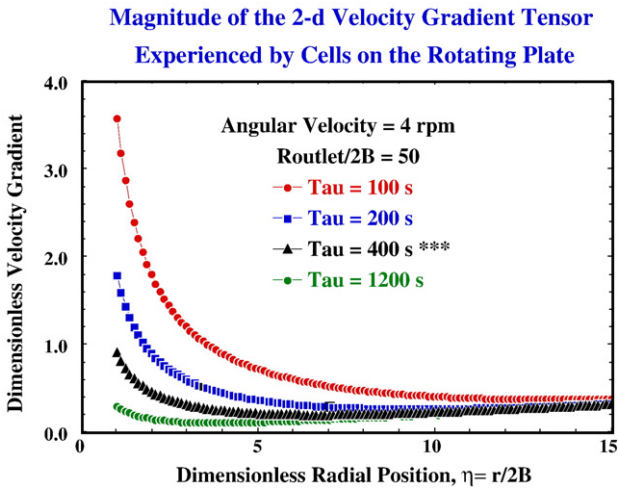

Fig. 2. Radial dependence of the magnitude of the dimensionless velocity gradient tensor $\Gamma(\eta)$ in the creeping flow regime, via Eq. (15), experienced by cells chemisorbed on the surface of the rotating plate at $z = 2B$. Residence time $\tau_{\text{Residence}}$ increases from the uppermost curve to the lowermost curve. All four curves converge at large radial position and scale linearly with η (i.e., exhibit positive linear dependence) due to tangential shear (i.e., $[\nabla v]_{z\Theta}$) at $z = 2B$ via rotation of the upper plate.

$$Re = \frac{\rho}{\mu} 2B \sqrt{v_\Theta^2(r = R_{\text{Plate}}, z = 2B) + \langle v_r(r = R_{\text{Plate}})\rangle^2}$$

$$= \frac{\rho}{\mu} 2B \sqrt{\{\Omega R_{\text{Plate}}\}^2 + \left\{\frac{Q_{\text{Volumetric}}}{4\pi B R_{\text{Plate}}}\right\}^2} \tag{18}$$

$$= \frac{\rho}{\mu}(2B)^2 \Omega \left\{\frac{R_{\text{Plate}}}{2B}\right\} \sqrt{1 + \left\{\frac{1}{2\Omega\tau_{\text{Residence}}}\right\}^2} < 1$$

For concentrated nutrient media that are approximately 5-fold more viscous than water at ambient temperature (i.e., $\mu/\rho \approx 5 \times 10^{-2}$ cm^2/s), gap thickness (i.e., $2B$) of 0.5 mm, plate diameter of 5 cm (i.e., $R_{\text{Plate}}/2B = 50$), angular velocity of 4 rpm, and residence time of 400 s, Eqs. (17) and (18) yield Reynolds numbers of 0.74 and 1.05, respectively.

2.9.6. Modified equations for nutrient consumption at the surface of the rotating plate via complex kinetics

It is necessary to modify the stress-free Damköhler number and the reaction/diffusion boundary condition at $z = 2B$ when the physiological aspects of heterogeneous nutrient consumption and subsequent cell proliferation are included in this analysis. All of the other equations remain unchanged, but a few additional parameters are required to characterize the inlet conditions at $r = R_{\text{inlet}}$, diffusivity ratios, association equilibrium constant for receptor-mediated cell–protein binding, and the cell–cell energy of attraction when receptors on adjacent protein sites form receptor complexes. If the stress-free rate of aerobic nutrient consumption by cells adhered to active protein sites on the surface of the rotating plate is;

$$-R_{A,\text{SurfaceRx}} = k_{\text{cell,Surface}}\{\rho_{\text{Nutrient}}\}_{z=2B}\{\rho_{\text{Oxygen}}\}_{z=2B}\Theta_{\text{Cell}}\Theta_{\text{Vacant}} \tag{19}$$

with dimensions of nutrient mass per area-time, then the dimensionless diffusion/reaction boundary condition at $z = 2B$, dimensionless kinetic rate law R^*_{Nutrient}, stress-free Damköhler number $\beta_{0,\text{Cells}}$, and nutrient/cell diffusion coefficient ratio $\delta_{\text{Diffusivity}}$ are defined in Eq. (20). Four Heaviside step functions exclude the stress-sensitive zeroth-order reaction rate from the boundary condition on the rotating plate when nutrients and oxygen do not exist within cells

under extreme diffusion-limited conditions. These step functions stipulate that cells and vacant cites must be present when aerobic proliferation is stimulated by viscous shear.

$$-\left\{\frac{\partial \Psi_{\text{Nutrient}}}{\partial \zeta}\right\}_{\zeta=1} = \beta_{0,\text{Cells}} R^{*}_{\text{Nutrient}}(\eta,\zeta=1) + H\{\Psi_{\text{Nutrient}}(\eta,\zeta=1)\}H\left\{\Psi_{\text{Oxygen}}(\eta,\zeta=1)\right\}H\{\Theta_{\text{Cell}}\}H\{\Theta_{\text{Vacant}}\}\beta_{\text{Stress}}\Gamma(\eta)$$

$$R^{*}_{\text{Nutrient}}(\eta,\zeta=1) = \Psi_{\text{Nutrient}}(\eta,\zeta=1)\Psi_{\text{Oxygen}}(\eta,\zeta=1)\Theta_{\text{Cell}}(\eta)\{1-\Theta_{\text{Cell}}(\eta)\}$$

$$\beta_{0,\text{Cells}} = \frac{2Bk_{\text{cell,Surface}}\{\kappa_{\text{Association}}\}^{\frac{1}{2}}\rho_{\text{Nutrient,Bulk}}(r=R_{\text{inlet}})}{D_{\text{Nutrient}}}$$

$$\delta_{\text{Diffusivity}} = \frac{D_{\text{Nutrient}}}{D_{\text{Cell}}} \tag{20}$$

The dimensionless temperature-dependent association equilibrium constant $\kappa_{\text{Association}}$ that characterizes receptor-mediated cell–protein interactions is;

$$\kappa_{\text{Association}} = 2BK_{\text{Cell}}\rho_{\text{Nutrient,Bulk}}(r=R_{\text{inlet}}) \tag{21}$$

2.10. Evaluation of bioreactor performance

The most effective bioreactor design depletes nutrients and proliferates cells most rapidly under physiological conditions, yielding the smallest bulk nutrient mass density at radial position r, averaged over the cross-sectional area for radial flow (i.e., $dS_{\text{Cross-Section}} = 2\pi r dz$). The velocity-weighted bulk nutrient mass density is defined as follows;

$$\rho_{\text{Nutrient,Bulk}}(r) = \frac{2\pi\int_{z=0}^{2B} v_r(r,z)\rho_{\text{Nutrient}}(r,z)r\,dz}{Q_{\text{Volumetric}}} = 6\int_{\zeta=0}^{1}\rho_{\text{Nutrient}}(r,\zeta)\{1-\zeta\}\zeta d\zeta \tag{22}$$

Numerical solutions of Eq. (13) are employed to calculate $\rho_{\text{Nutrient,Bulk}}$ via Eq. (22). Results are presented in Figs. 3–5,8. If the separation-of-variables solution for $\Psi_{\text{Nutrient}}(\eta,\zeta)$, given by Eq. (14), is valid, then bulk nutrient mass density [i.e., Eq. (22)] scales as $\exp(-\eta^2/Pe_{\text{MT}})$.

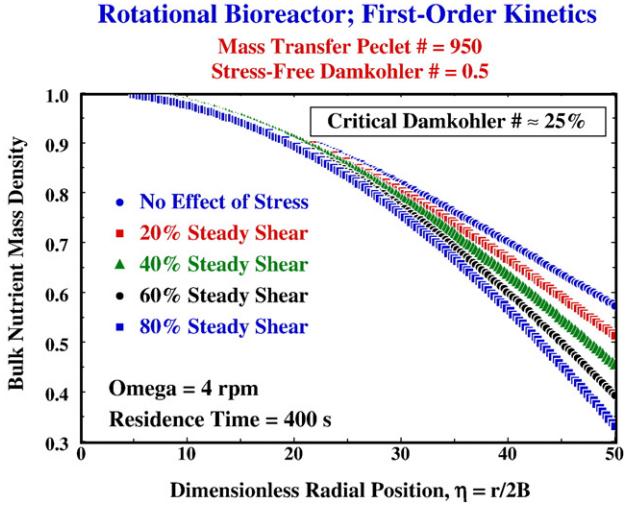

Fig. 3. Dimensionless bulk nutrient mass density profiles in continuous-flow rotational bioreactors at various stress-sensitive Damköhler numbers with 1st-order irreversible stress-free nutrient consumption that depends only on nutrient mass density near the surface of the rotating plate. The legend should be interpreted as the ratio of the stress-sensitive Damköhler number to the stress-free Damköhler number. This ratio increases from the uppermost curve to the lowermost curve, with no angular velocity modulations (i.e., $A=0$). Parameters: dimensionless step size in the z-direction, $\Delta\zeta=0.010$; dimensionless step size in the radial direction, $\Delta\eta=0.288$ (i.e., $\Delta r/R_{\text{Plate}}\approx 5.77\times10^{-3}$).

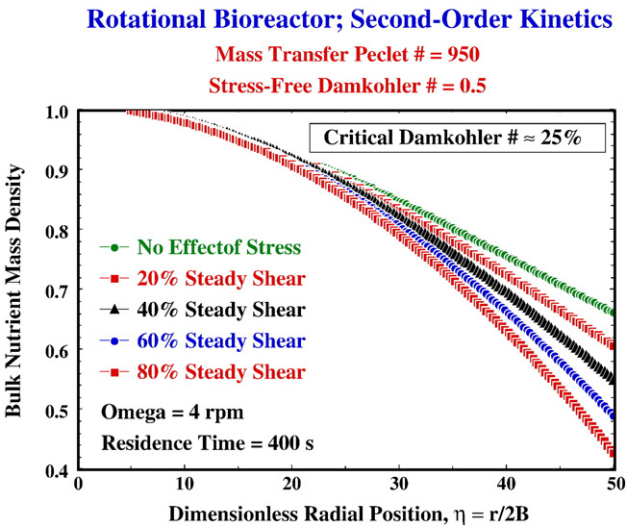

Fig. 4. Dimensionless bulk nutrient mass density profiles in continuous-flow rotational bioreactors at various stress-sensitive Damköhler numbers with 2nd-order irreversible stress-free nutrient consumption that depends only on nutrient mass density near the surface of the rotating plate. The legend should be interpreted as the ratio of the stress-sensitive Damköhler number to the stress-free Damköhler number. This ratio increases from the uppermost curve to the lowermost curve, with no angular velocity modulations (i.e., $A=0$). Parameters: dimensionless step size in the z-direction, $\Delta\zeta=0.010$; dimensionless step size in the radial direction, $\Delta\eta=0.288$ (i.e., $\Delta r/R_{\text{Plate}}\approx 5.77\times10^{-3}$).

$$\rho_{\text{Nutrient,Bulk}}(r)\approx\rho_{\text{Nutrient,Bulk}}(r=R_{\text{inlet}})\exp\left\{-\frac{\chi^2}{12Pe_{\text{MT}}}\eta^2\right\}\int_{\zeta=0}^{1}G(\zeta)\{1-\zeta\}\zeta d\zeta \tag{23}$$

2.11. Computer simulations

2.11.1. Effect of the stress-sensitive Damköhler number on nutrient consumption for first-order and second-order irreversible stress-free kinetics

Bulk nutrient mass density profiles as a function of distance r from the rotation axis were generated at constant values of the mass transfer Peclet number (i.e., $Pe_{\text{MT}}=ReSc=950$) and stress-free Damköhler number (i.e., $\beta_{0,n\text{th-order}}=0.5$). For stress-free nth-order irreversible chemical kinetics (i.e., $n=1,2$), this combination of Pe_{MT} and $\beta_{0,n\text{th-order}}$ corresponds to the following relation between nutrient residence time $\tau_{\text{Residence}}$ and the characteristic time constant for nth-order chemical reaction $\omega_{\text{ChemicalRx}}$;

$$\frac{Pe_{\text{MT}}}{\beta_{0,n\text{th}-\text{order}}} = \frac{\omega_{\text{ChemicalRx}}\left\{\frac{R_{\text{Plate}}}{2B}\right\}^2}{2\tau_{\text{Residence}}} = 1900 \tag{24}$$

where $\tau_{\text{Residence}}$ and $\omega_{\text{ChemicalRx}}$ (i.e., for simple nth-order nutrient consumption) are defined as;

$$\tau_{\text{Residence}} = \frac{2\pi BR^2_{\text{Plate}}}{Q_{\text{Volumetric}}};\ \omega_{\text{ChemicalRx}} = \frac{2B}{k_{n,\text{Surface}}\left\{\rho_{\text{Nutrient,Bulk}}(r=R_{\text{inlet}})\right\}^{n-1}} \tag{25}$$

Rotation of the upper plate does not affect the residence time because $\tau_{\text{Residence}}$ is based on replenishment of the total volume

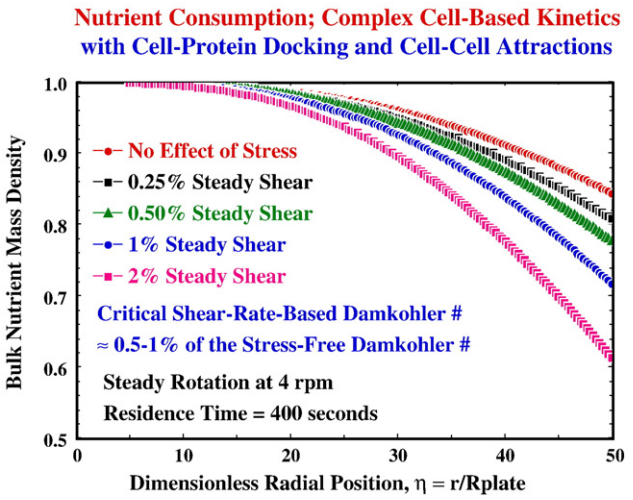

Fig. 5. Dimensionless bulk nutrient mass density profiles in continuous-flow rotational bioreactors at various stress-sensitive Damköhler numbers with complex rates of stress-free nutrient consumption. The % steady shear indicated in the legend should be interpreted as the ratio of the stress-sensitive Damköhler number to the stress-free Damköhler number. This ratio increases from the uppermost curve to the lowermost curve, with no angular velocity modulations (i.e., $A=0$). Parameters; mass transfer Peclet number = 200; stress-free Damköhler number = 2.5; steady angular velocity of rotating plate = 4 rpm; residence time = 400 s; dimensionless step size in the z-direction, $\Delta\zeta=0.010$; dimensionless step size in the radial direction, $\Delta\eta=0.292$ (i.e., $\Delta r/R_{\text{Plate}}\approx 5.84\times10^{-3}$); Hill coefficient, $1/\lambda=1$; association equilibrium constant for receptor-mediated cell–protein binding, $\kappa_{\text{Association}}=0.50$; cell–cell attractive interaction energy, $\varphi=-0.50$; nutrient molecular weight = 1000 Da; nutrient-cell diffusivity ratio, $\delta_{\text{Diffusivity}}=D_{\text{Nutrient}}/D_{\text{Cell}}=3$; inlet mass ratio of oxygen to nutrients, $\rho_{\text{Oxygen}}(r=R_{\text{inlet}})/\rho_{\text{Nutrient}}(r=R_{\text{inlet}})=0.07$ (i.e., 7%); mass ratio of cells seeded on the surface of the rotating plate at $r=R_{\text{inlet}}$ to nutrients in the inlet stream, $\rho_{\text{Cell}}(r=R_{\text{inlet}})/\{2B\rho_{\text{Nutrient}}(r=R_{\text{inlet}})\}=0.10$ (i.e., 10%); ratio of mass of oxygen consumed to mass of nutrients consumed by cells adhered on protein-coated surface, $\varepsilon_{\text{Oxygen}}/\varepsilon_{\text{Nutrient}}=0.04$ (i.e., 4%); ratio of mass of cells produced to mass of nutrients consumed by cells adhered on protein-coated surface, $\varepsilon_{\text{Cell}}/\varepsilon_{\text{Nutrient}}=0.25$ (i.e., 25%).

of fluid in the bioreactor via volumetric flowrate $Q_{\text{Volumetric}}$, not simply the time required for fluid parcels to travel from R_{inlet} to R_{outlet} via streamlines that exhibit more spiral-like characteristics at higher angular velocity Ω. When the upper limit of the dimensionless radial coordinate is $R_{\text{Plate}}/\{2B\}=50$ on the right side of Fig. 3 for 1st-order stress-free kinetics, this corresponds to a residence time $\tau_{\text{Residence}}$ that is ≈66% of the characteristic time constant for chemical reaction, $\omega_{\text{ChemicalRx}}$. The shape of these bulk nutrient mass density profiles, given by Eq. (23), depends strongly on the fact that position-dependent (i) shear, described by $\Gamma(\eta)$, and (ii) active differential surface area for anchorage-dependent cells increase linearly at larger distances r from the rotation axis. The critical stress-sensitive Damköhler number is slightly larger than 20% of the stress-free Damköhler number in Fig. 3, certainly less than 40% of $\beta_{0,\text{ 1st-order}}$.

Reasonable stress-free nutrient consumption (i.e., ≈42%) by anchorage-dependent cells is predicted for 1st-order kinetics in Fig. 3 when $R_{\text{Plate}}/\{2B\}=50$ and $\tau_{\text{Residence}}\approx 0.66\omega_{\text{ChemicalRx}}$. This outlet conversion for 2-dimensional creeping flow rotational bioreactors matches the predictions for stress-free nutrient consumption in 1-dimensional laminar flow tubular bioreactors [22] when the important time constants and dimensionless numbers assume the numerical values summarized in Table 1. If the gap thickness (i.e., $2B$) between the stationary and rotating plates, instead of the outer plate radius, is used to define Pe_{MT} in this rotational bioreactor investigation, then approximately 42% stress-free nutrient consumption via 1st-order kinetics is achieved when (i) $Pe_{\text{MT}}/\beta_{0,\text{1st-order}}\approx 38$ with $\tau_{\text{Residence}}\approx 0.66\omega_{\text{ChemicalRx}}$ for position-dependent steady shear in 2-dimensional creeping flow rotational bioreactors, and (ii) $Pe_{\text{MT}}/\beta_{0,\text{1st-order}}\approx 50$ with $\tau_{\text{Residence}}\approx 0.80\omega_{\text{ChemicalRx}}$ for constant shear in 1-dimensional laminar flow tubular bioreactors.

Tubular Bioreactor Parameters

$$Pe_{\text{MT}}=\frac{\langle v_z\rangle_{\text{Average}}R_{\text{wall}}}{D_{\text{Nutrient}}}=50;\quad \beta_{0,n\text{th}-\text{order}}=\frac{k_{n,\text{Surface}}R_{\text{wall}}\left\{\rho_{\text{Nutrient,Bulk}}(z=0)\right\}^{n-1}}{D_{\text{Nutrient}}}=1$$
$$\omega_{\text{ChemicalRx}}=\frac{R_{\text{wall}}}{2k_{n,\text{Surface}}\left\{\rho_{\text{Nutrient,Bulk}}(z=0)\right\}^{n-1}};\quad \tau_{\text{Residence}}=\frac{L_{\text{PFR}}}{\langle v_z\rangle_{\text{Average}}}=0.8\omega$$
$$\frac{Pe_{\text{MT}}}{\beta_{0,n\text{th}-\text{order}}}=\frac{2\omega_{\text{ChemicalRx}}}{\tau_{\text{Residence}}}\left\{\frac{L_{\text{PFR}}}{R_{\text{wall}}}\right\}=50 \tag{26}$$

For 2nd-order irreversible stress-free kinetics, the time constant ratios and dimensionless parameters summarized in Table 1 yield ≈33–34% nutrient consumption in both types of bioreactors. Less nutrient consumption is predicted for stress-free 2nd-order irreversible kinetics in Fig. 4 relative to stress-free 1st-order kinetics in Fig. 3. This occurs because only one event is required for stress-free consumption via 1st-order kinetics, based on the presence of nutrients near the surface of the rotating plate where anchorage-dependent cells are bound to active protein sites. Two events must occur simultaneously for stress-free consumption via 2nd-order kinetics. Even though the critical Damköhler number is reported rather subjectively for 1st-order nutrient consumption in Fig. 3, bulk nutrient mass density profiles seem to be outside of the range of experimental uncertainty when the stress-sensitive Damköhler number is slightly larger than 20% of the stress-free Damköhler number. A similar conclusion is obtained for simple 2nd-order kinetics in Fig. 4. Except for reaction order n, all other dimensionless parametric values are identical in Fig. 3 (i.e., $n=1$) and Fig. 4 (i.e., $n=2$).

2.11.2. Complex rates of stress-free nutrient consumption

These simulations require the declaration of several dimensionless parameters, due to the complexity of the kinetic rate law that describes stress-free nutrient consumption. The last entry in Table 1 reveals that it is necessary to increase the ratio of the stress-free Damköhler number relative to the mass transfer Peclet number from ≈0.05% in Figs. 3 and 4, to >1% in Fig. 5, to achieve reasonable conversion of nutrients when the upper limit of the dimensionless radial coordinate is $R_{\text{Plate}}/\{2B\}=50$ on the right side of the graph in Fig. 5. Bulk nutrient mass density profiles in Fig. 5 suggest that the system is extremely sensitive to viscous shear at the cell/aqueous-medium interface when stress-free nutrient consumption is modelled as a cascade of four sequential events, according to Eq. (19). Qualitative inspection suggests that the critical stress-sensitive Damköhler number in Fig. 5 corresponds to 0.5–1% steady shear. Recent studies

Table 1
Tubular and rotational bioreactor parameters that yield equivalent stress-free nutrient consumption in the exit stream via simple nth-order and complex kinetics.

Parameters	Tubular bioreactor 1-d laminar flow [22]	Rotational bioreactor 2-d creeping flow
Mass transfer Peclet number	50	950
Stress-free Damköhler number	1	0.5
Length scale ratio	$L_{\text{PFR}}/R_{\text{wall}}=20$	$R_{\text{Plate}}/\{2B\}=50$
Time constant ratio	$\tau_{\text{Residence}}/\omega_{\text{ChemicalRx}}=0.80$	$\tau_{\text{Residence}}/\omega_{\text{ChemicalRx}}=0.66$
Stress-free nutrient conversion; 1st-order kinetics (i.e., $n=1$)	43%	42%
Stress-free nutrient conversion; 2nd-order kinetics (i.e., $n=2$)	33%	34%
Stress-free nutrient conversion; complex heterogeneous kinetics	<1%	<1%

Tubular bioreactor parameters are defined above in Eq. (26) for simple nth-order kinetics, and the corresponding rotational bioreactor parameters are defined above via Eqs. (12), (24), and (25).
See the caption to Fig. 5 for numerical values of all rotational bioreactor parameters when the complex stress-free rate of nutrient consumption is given by Eq. (19).

Table 2
Tubular and rotational bioreactor parameters that yield equivalent stress-free nutrient consumption in the exit stream via complex heterogeneous kinetics.

Parameters	Tubular bioreactor 1-d laminar flow [22]	Rotational bioreactor 2-d creeping flow
Mass transfer Peclet number	10	200
Stress-free Damköhler number	5	2.5
Length scale ratio	$L_{PFR}/R_{wall}=20$	$R_{Plate}/\{2B\}=50$
Time constant ratio	$\tau_{Residence}/\omega_{ChemicalRx}=20$	$\tau_{Residence}/\omega_{ChemicalRx}\approx 16$
Stress-free nutrient conversion	**15%	16%

See the caption to Fig. 5 for numerical values of all rotational bioreactor parameters when the stress-free rate of nutrient consumption is given by Eq. (19).
**Due to a computational error, predictions of stress-free nutrient consumption via complex heterogeneous kinetics have been overestimated in Fig. 4 of reference [22]. Based on the parameters in Table 2 for tubular bioreactors, correct predictions of viscous shear on nutrient consumption at the tube outlet are summarized as follows; 0.25% steady shear yields 22% nutrient conversion, 0.50% steady shear yields 28% conversion, and 1% steady shear yields 38% conversion. All of these predictions have been overestimated in Fig. 4 of reference [22], but the trends are correct.

of fluid flow in and around 3-dimensional scaffolds, with average velocities between 10^{-3} cm/s and 10^{-2} cm/s that correspond to maximum wall shear stresses on the order of 3×10^{-2} Pa, describe extensive proliferation of osteoblast-like cells [23]. Time constant ratios and dimensionless parameters for tubular and rotational bioreactors are summarized in Table 2 to achieve equivalent stress-free nutrient consumption in the exit stream via complex cell-based kinetics.

2.12. Non-reversing dynamic shear via modulated rotation of the upper plate at $z=2B$ with 2-dimensional creeping flow

Unidirectional oscillatory motion of the rotating plate simulates pulsatile stress on anchorage-dependent cells. The strategy to introduce physiological viscous shear into rotational bioreactors is accomplished by adding a dynamic component to steady shear [24] such that the time-dependent *unidirectional* angular displacement $\phi(t)$ and *non-reversing* angular velocity $d\phi/dt$ of the rotating plate are expressed as follows;

$$\begin{aligned}\phi(t) &= \Omega t + \frac{1}{2}A\left\{t - \frac{\sin(\omega_{Heart}t)}{\omega_{Heart}}\right\}\\ \frac{d\phi}{dt} &= \Omega + A\sin^2\left(\frac{1}{2}\omega_{Heart}t\right)\end{aligned} \tag{27}$$

where frequency $\omega_{Heart}=2\pi\upsilon_{Heart}$ (i.e., $\upsilon_{Heart}\approx1$ cycle/s) is the dominant frequency in the power spectrum when one considers the coupling between cardiac and respiratory oscillators superimposed on random noise [25]. The volume of blood displaced per heartbeat is proportional to the peak-to-peak amplitude A ([=] radians/second) of dynamic angular velocity modulations [26], superimposed on steady shear due to Ω. The upper limit of the peak-to-peak amplitude of these modulations (i.e., $A\approx0.42$ rad/s) is limited by the requirement to maintain creeping flow [see Eq. (33) and Table 3]. Unidirectional motion of the rotating plate is guaranteed by the functional form of $d\phi/dt$ in Eq. (27). Hence, anchorage-dependent cells always experience tangential viscous shear forces in the positive tangential direction in cylindrical coordinates (i.e., Θ-direction). Recent studies of steady, pulsatile, and oscillatory fluid flow in perfusion bioreactors [27] suggest that osteoblasts are stimulated and cell viability is maintained when the peak-to-peak amplitude of the time-dependent flowrate is similar in magnitude to the steady flowrate, at 1 or 2 Hz. These conditions are employed in Fig. 6, such that $A\approx\Omega$ at 1 Hz.

This dynamic rotational bioreactor exhibits similarities to pulsatile flow and *unidirectional* viscous shear in tubes. The combination of steady and dynamic rotation of the solid plate at $z=2B$ induces tangential fluid motion via Eq. (28);

$$v_\Theta(r,z,t) = f(r)g(z)\frac{d\phi}{dt} \tag{28}$$

where $f(r)$ and $g(z)$ have been discussed earlier via Eq. (6), assuming that the upper plate is in a *state of pure rotation*. Unless one seeks viscoelastic information associated with harmonic motion of the rotating plate, it is not necessary to describe modulations in angular displacement, angular velocity of the rotating plate, or the tangential linear fluid velocity component via $\exp\{i\omega t\}$, with subsequent analysis of the real and imaginary responses. Hence, dynamic fluid motion with continuous radial flow that simulates physiological viscous shear is described as follows;

$$\begin{aligned}v_\Theta(r,z,t) &= \frac{rz}{2B}\left[\Omega + A\sin^2\left(\frac{1}{2}\omega_{Heart}t\right)\right]\\ v_r(r,z) &= \frac{3Q_{Volumetric}}{8\pi B^2}\frac{z}{r}\left\{2-\frac{z}{B}\right\}\\ \langle v_r(r=R_{Plate})\rangle &= \frac{Q_{Volumetric}}{4\pi BR_{Plate}}\end{aligned} \tag{29}$$

The functions described by Eqs. (27)–(29) satisfy all components of the creeping flow Equation of Motion, and the important boundary condition on the surface of the rotating plate. The viscous nature of the nutrient medium will introduce an oscillatory time lag in response to the harmonic disturbance that could be quantified via implementation of the "$\exp\{i\omega t\}$-method" and consideration of $\rho\partial v_\Theta/\partial t$ on the left side of the Θ-component of the Equation of Motion. The importance of $\rho\partial v_\Theta/\partial t$ relative to viscous forces due to $\tau_{z\Theta}$ (i.e., oscillatory forces that produce an accumulation of momentum relative to forces due to viscous momentum flux) scales as the product of the Reynolds and Strouhal numbers, which reduces to $4\omega B^2/(\mu/\rho)\approx0.1\pi$ for this rotational bioreactor using the parameters described in the footnote to Table 3 (i.e., volume-to-active-surface-area $=2B$, is chosen as the characteristic length). Modulations in the angular velocity of the rotating

Table 3
Dependence of the Reynolds number for 2-dimensional flow in rotational bioreactors on the peak-to-peak amplitude A of angular velocity modulations for the tangential velocity component v_Θ.

A [rad/s]	0	0.25	0.42	0.50	0.75	1.00
Reynolds #	1.05	1.36	1.57	1.67	1.98	2.30

Parameters; $2B=0.5$ mm, $R_{Plate}=2.5$ cm, $\Omega=0.42$ rad/s, $\omega_{Heart}=2\pi$ rad/s, $\tau_{Residence}=400$ s, $\mu/\rho=5\times10^{-2}$ cm^2/s.

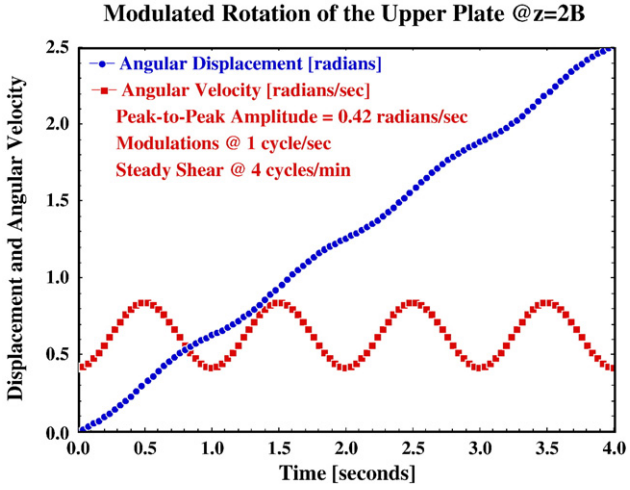

Fig. 6. Time-dependent angular displacement $\phi(t)$ and angular velocity $d\phi/dt$ of the rotating plate at $z=2B$, simulating pulsatile flow in rotational bioreactors that exhibit steady and dynamic shear. Parametric values; $\Omega\approx0.42$ rad/s (i.e., 4 rpm), $\omega_{Heart}=2\pi$ rad/s, peak-to-peak amplitude of angular velocity modulations $A=0.42$ rad/s.

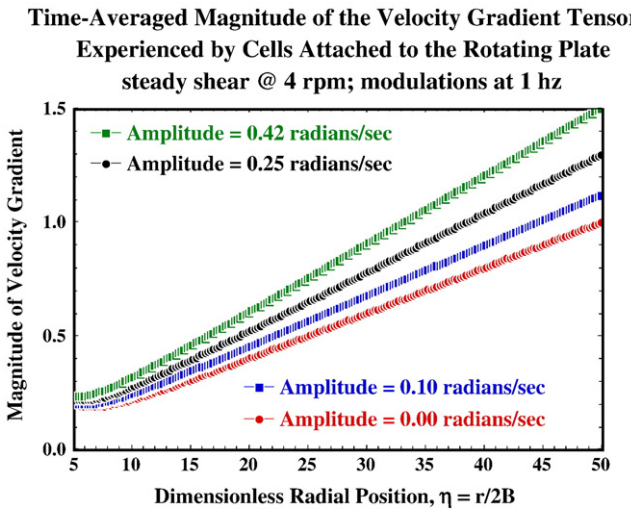

Fig. 7. Effect of the amplitude of peak-to-peak angular velocity modulations A on the time-averaged position-dependent magnitude of the dimensionless velocity gradient tensor experienced by cells attached to the surface of the rotating plate at $z=2B$. This peak-to-peak amplitude A increases from the lowermost curve to the uppermost curve. Parametric values; $\Omega \approx 0.42$ rad/s (i.e., 4 rpm), $\omega_{Heart}=2\pi$ rad/s, residence time $\tau_{Residence}=400$ s, $R_{inlet}/2B=5$, $R_{outlet}/2B=50$.

plate affect the $r\Theta$-, Θr-, and $z\Theta$-elements of the velocity gradient tensor, according to Eq. (30);

$$\begin{aligned}
\{[\nabla v]_{zr}\}_{z=2B} &= \left\{\frac{\partial v_r}{\partial z}\right\}_{z=2B} = -\frac{3Q_{Volumetric}}{4\pi B^2 r}\\
\{[\nabla v]_{z\Theta}\}_{z=2B} &= \left\{\frac{\partial v_\Theta}{\partial z}\right\}_{z=2B} = \frac{r}{2B}\left[\Omega + A\sin^2\left(\frac{1}{2}\omega_{Heart}t\right)\right]\\
\{[\nabla v]_{r\Theta}\}_{z=2B} &= \left\{\frac{\partial v_\Theta}{\partial r}\right\}_{z=2B} = \Omega + A\sin^2\left(\frac{1}{2}\omega_{Heart}t\right)\\
\{[\nabla v]_{\Theta r}\}_{z=2B} &= \left\{\frac{1}{r}\frac{\partial v_r}{\partial \Theta} - \frac{v_\Theta}{r}\right\}_{z=2B} = -\Omega - A\sin^2\left(\frac{1}{2}\omega_{Heart}t\right)
\end{aligned} \tag{30}$$

The fluctuating position-dependent magnitude of the velocity gradient tensor in Eq. (31) selects only those elements that act across the surface where cells are attached;

$$|\nabla v(r,t)|_{z=2B} = \sqrt{\frac{1}{2}\{\nabla v\}:\{\nabla v\}^T} \overset{\text{select nonzero scalar elements that act across the surface at } z=2B}{\Rightarrow} \sqrt{\frac{1}{2}\left[\left\{\frac{r}{2B}\right\}^2\left\{\Omega + A\sin^2\left(\frac{1}{2}\omega_{Heart}t\right)\right\}^2 + \left\{\frac{3Q_{Volumetric}}{4\pi B^2 r}\right\}^2\right]} \tag{31}$$

Steady and dynamic rotation of the upper plate must be restricted to ensure that the creeping flow requirement is satisfied at $z=2B$ and $r=R_{Plate}$. Upon implementing a time-averaging procedure over one cycle of angular velocity modulations to estimate the tangential velocity component, the Reynolds number is constructed in terms of the magnitude of the velocity vector;

$$Re = \frac{\rho}{\mu}2B\sqrt{\langle v_r(r=R_{Plate})\rangle^2 + \frac{\omega_{Heart}}{2\pi}\int_0^{\frac{2\pi}{\omega_{Heart}}} v_\Theta^2(r=R_{Plate},z=2B,t)\,dt} \tag{32}$$

Table 3 summarizes the effect of the peak-to-peak amplitude of angular velocity modulations in v_Θ via Eq. (29) on the Reynolds number in Eq. (32).

Hence, one predicts Reynolds numbers on the order of unity when the peak-to-peak amplitude A of angular velocity modulations at 1 Hz is the same as the magnitude of the angular velocity for steady rotation (i.e., $\Omega=0.42$ rad/s).

2.13. Dynamic bioreactor analysis via time-averaging of the periodic boundary condition on the surface of the rotating plate at $z=2B$

Modulations of the rotating plate that simulate physiological viscous shear introduce time dependence into (i) the magnitude of the velocity gradient tensor, as given by Eq. (31), and (ii) the reaction/diffusion boundary condition at the active surface. Unless one considers $\partial\rho_{Nutrient}/\partial t$ in Eq. (10), there is no explicit time dependence in the mass transfer equation because the tangential velocity component (i.e., v_Θ) does not contribute to convective transport as a consequence of angular symmetry, effectively eliminating angular coordinate Θ as an independent variable [20] in this analysis. The position-dependent magnitude of the dimensionless velocity gradient tensor on the surface of the rotating plate is time-averaged over one cycle of oscillation in Eq. (33), retaining contributions from angular velocity modulations in this bioreactor simulation of cardiovascular dynamics [26]. All of the required boundary conditions for simple nth-order nutrient consumption are summarized below,

$$\begin{aligned}
&\Psi_{Nutrient} = 1 @ \eta = \eta_{start}, 0 \le \zeta < 1\\
&\left\{\frac{\partial \Psi_{Nutrient}}{\partial \zeta}\right\}_{\zeta=0} = 0\\
&-\left\{\frac{\partial \Psi_{Nutrient}}{\partial \zeta}\right\}_{\zeta=1} = \beta_{0,nth-order}\Psi^n_{Nutrient}(\eta,\zeta=1) + H\{\Psi_{Nutrient}(\eta,\zeta=1)\}\beta_{Stress}\langle\Gamma(\eta,t)\rangle_{time-averaged}\\
&\langle\Gamma(\eta,t)\rangle_{time-averaged} = \frac{\langle|\nabla v(r,t)|_{z=2B}\rangle_{time-averaged}}{|\nabla v(r=R_{Plate};A=0)|_{z=2B}}\\
&= \frac{\frac{\omega_{Heart}}{2\pi}\int_0^{\frac{2\pi}{\omega_{Heart}}}\left[\eta^2\left\{\Omega + A\sin^2\left(\frac{1}{2}\omega_{Heart}t\right)\right\}^2 + \left\{\frac{3}{\tau_{Residence}}\left(\frac{R_{Plate}}{2B}\right)^2\right\}^2\frac{1}{\eta^2}\right]^{\frac{1}{2}}dt}{\frac{R_{Plate}}{2B}\sqrt{\Omega^2 + \left\{\frac{3}{\tau_{Residence}}\right\}^2}}
\end{aligned} \tag{33}$$

The radial dependence of $\langle\Gamma(\eta,t)\rangle_{time-averaged}$ from inlet to outlet of the parallel-disk configuration is illustrated in Fig. 7 under creeping flow conditions.

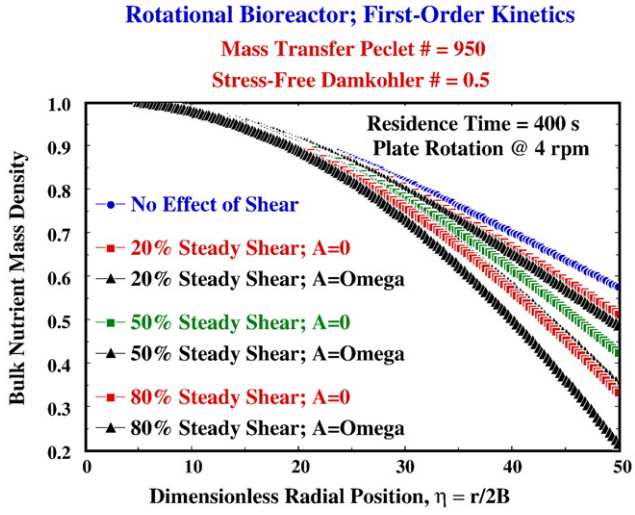

Fig. 8. Dimensionless bulk nutrient mass density profiles in continuous-flow rotational bioreactors that include the effects of steady and time-averaged non-reversing dynamic shear in the reaction/diffusion boundary condition on the surface of the rotating plate at $z=2B$. Stress-free nutrient consumption follows 1st-order irreversible kinetics that depend only on nutrient mass density at the surface of the rotating plate. The legend should be interpreted as the ratio of the stress-sensitive Damköhler number to the stress-free Damköhler number, and this ratio increases from the uppermost curve to the lowermost curve. The effect of non-reversing dynamic shear superimposed on steady shear is operative when the peak-to-peak amplitude A of angular velocity modulations at 1 Hz matches the magnitude of steady shear (i.e., $A=\Omega$). Predictions for 50% steady shear with angular velocity modulations are barely visible above the predictions for 80% steady shear without angular velocity modulations. Parameters: dimensionless step size in the z-direction, $\Delta\zeta=0.010$; dimensionless step size in the radial direction, $\Delta\eta=0.288$ (i.e., $\Delta r/R_{Plate}\approx 5.77\times10^{-3}$).

Relative to position-dependent steady-shear conditions in the lowermost curve of Fig. 7, the magnitude of the time-averaged "shear rate" experienced by cells attached to the rotating plate increases by approximately 50% when the peak-to-peak amplitude A of angular velocity modulations matches the steady-shear angular velocity of 0.42 rad/s.

2.14. Effect of steady and non-reversing dynamic shear on nutrient consumption via first-order stress-free kinetics

Bulk nutrient mass density profiles, with and without dynamic shear induced by angular velocity modulations of the upper plate, are illustrated in Fig. 8 as a function of dimensionless radial position, $\eta = r/\{2B\}$, from the rotation axis for 1st-order stress-free nutrient consumption. The analogous profiles in Fig. 3 without dynamic shear suggest that the critical stress-sensitive Damköhler number is approximately 25% of the stress-free Damköhler number.

Nutrient profiles with and without dynamic shear in Fig. 8 are essentially indistinguishable when the stress-sensitive Damköhler number is only 20% of the stress-free Damköhler number. However, significantly increased nutrient consumption occurs in the presence of dynamic shear when the stress-sensitive Damköhler number is either 50% or 80% of the stress-free Damköhler number. When the peak-to-peak amplitude A of angular velocity modulations is similar to the steady shear angular velocity Ω, one concludes that the effect of time-averaged non-reversing dynamic shear in these 2-dimensional creeping flow rotational bioreactors is not significant unless one is above the critical value of the stress-sensitive Damköhler number that has been identified under steady shear conditions.

2.15. Unusual characteristics of this bioreactor analysis

There are several aspects of this investigation that deviate significantly from the traditional design of ordinary chemical reactors. (1) Kinetic rate expressions that describe nutrient consumption are modified for stress-sensitive reactions, based on the formalism of scalar cross-phenomena in the thermodynamics of irreversible processes. (2) The adsorption isotherm for receptor-mediated cell binding to protein-coated surfaces, based on cell mass density in the vicinity of the active surface rather than in the mass transfer boundary layer or in the bulk aqueous medium, is modified to account for attraction between cells on adjacent protein sites and the formation of receptor complexes. (3) Since stress-enhanced nutrient consumption occurs at the cell/aqueous-medium interface, only those elements of the velocity gradient tensor, $[\nabla v]_{zr}$ and $[\nabla v]_{z\Theta}$, that act across the surface of the rotating plate are included in the stress-sensitive reaction rate. (4) Stress-sensitive zeroth-order contributions to the rate of nutrient consumption are quenched via Heaviside step functions when cells are starved of either nutrients or oxygen due to extreme diffusion-controlled conditions within the mass transfer boundary layer adjacent to the active surface. (5) Surface diffusion of newly produced biomass within the aqueous protein coating on the rotating plate, strongly influenced by viscous shear in the radial direction, is invoked to relate cell mass density on the surface to nutrient mass density in the mass-transfer boundary layer adjacent to the rotating plate. (6) Angular symmetry is invoked to neglect convective mass transfer in the Θ-direction, even though there is a significant contribution to tangential flow via rotation of the upper plate. (7) Non-reversing angular velocity modulations of the upper plate simulate pulsatile cardiovascular flow and introduce time-dependence in the reaction/diffusion boundary condition at the active surface that has been averaged over one cycle of oscillation. (8) The complete problem description is developed in terms of mass density, not molar density, because cell physiology and the cascade of events that describe nutrient consumption are treated phenomenologically via the analogy with heterogeneous catalysis.

3. Conclusions

Theoretical analysis and computer simulations of continuous-flow rotational bioreactors at low Reynolds numbers are described from the viewpoint of stress-free and stress-sensitive nutrient consumption. Estimates of the mass of biomass produced per total mass of nutrients consumed (i.e., $\varepsilon_{Cell}/\varepsilon_{Nutrient} \approx 25\%$) are reasonable, based on experimental data for several glucose-fed micro-organisms [28,29]. All microscopic solutions that were generated in this investigation exhibit internal self-consistency and satisfy a quasi-macroscopic version of the nutrient mass balance to within 0.1%, via the ratio of the left-side to the right-side of the following equation that is applicable for incompressible fluids with constant physical properties at high mass transfer Peclet numbers, such that radial diffusion is negligible relative to convective transport of nutrients in the radial direction;

$$-\frac{d\Psi_{Nutrient,Bulk}}{d\eta} = \frac{\eta}{Pe_{MT}}\left[\beta_{0,Cells}R^{*}_{Nutrient}(\eta,\zeta=1) + \beta_{Stress}\langle\Gamma(\eta,t)\rangle_{time-averaged}\right] \quad (34)$$

The dimensionless magnitude of the position-dependent velocity gradient tensor at the cell/aqueous-medium interface (i.e., Γ) is calculated via Eq. (15) for steady rotation and Eq. (33) when modulated rotation of the upper plate is implemented to simulate pulsatile cardiovascular viscous shear at physiological frequencies. These rotational bioreactors must operate above the critical stress-sensitive Damköhler number, identified under steady shear conditions, before dynamic shear has a distinguishable effect on bioreactor performance. The critical stress-sensitive Damköhler number is approximately 25% of the stress-free Damköhler number (i.e., $\beta_{0,n\text{th-order}} = 0.5$) for simple nth-order rates of nutrient consumption (i.e., $n = 1,2$), and approximately 0.5–1% of the stress-free Damköhler number (i.e., $\beta_{0,Cells} = 2.5$) for complex rates of nutrient consumption that require the presence of nutrients, oxygen, anchored cells, and vacant active sites in the aqueous protein layer on the rotating plate. In general, bioreactor designs must consider mechano-sensitive zeroth-order contributions to the overall rate of nutrient consumption when the shear-rate-based Damköhler number exceeds its critical value.

Nomenclature

A	peak-to-peak amplitude of angular velocity modulations of the rotating plate at $z = 2B$ (i.e., $A \leq 0.42$ rad/s)
B	one-half of the gap thickness between the stationary and rotating plates
D_{Cell}	surface diffusion coefficient for cells on protein-coated surfaces; length^2/time
$D_{Nutrient}$	ordinary molecular diffusion coefficient of nutrients in aqueous mixtures; length^2 per time
D_{Oxygen}	ordinary molecular diffusion coefficient of dissolved oxygen in the aqueous medium; length^2 per time
$F(\eta)$	radial part of the separation-of-variables solution for dimensionless nutrient mass density, $\Psi_{Nutrient}(\eta,\zeta)$
g	velocity gradient tensor (i.e., ∇v)
g_{ij}	ij-element of the velocity gradient tensor, evaluated at the rotating plate, which is not symmetric; $g_{ij} \neq g_{ji}$
$g_{i,ForceField}$	force per unit mass exerted on species i due to the gravitational field
$G(\zeta)$	parabolic cylinder functions; axial (i.e., z) part of the separation-of-variables solution for dimensionless nutrient mass density that satisfies Weber's differential equation
$H(x)$	Heaviside step function
$j_{A,Diffusion}$	diffusional mass flux of species A; dimensions of species mass per area-time
$k_{n,Surface}$	kinetic rate constant for stress-free heterogeneous rate of nutrient consumption via simple nth-order reaction that

depends only on nutrient mass density at the surface of the rotating plate; {volume/mass}$^{n-1}$·length/time

$k_{cell,Surface}$ kinetic rate constant for stress-free heterogeneous rate of nutrient consumption based on complex cell-based kinetics; {volume/mass}·length/time

K_{cell} adsorption/desorption (i.e., association) equilibrium constant; cm^2/g

L_{PFR} length of an analogous plug-flow tubular bioreactor

MW_i molecular weight of species i

Pe_{MT} mass transfer Peclet number based on radial flow in rotational bioreactors

$q_{Conduction}$ molecular flux of thermal energy; dimensions of energy per area-time

$Q_{Volumetric}$ volumetric flowrate of the culture medium radially outward between the plates

r independent radial variable, measured in the flow direction that elutes nutrients from the rotating bioreactor

Δr step size in the radial direction, between grid points

$-R_{A,SurfaceRx}$ stress-free heterogeneous rate of nutrient consumption; mass per area-time

R_{inlet} radial position on the rotating plate where fresh nutrients enter the bioreactor

R_{Plate} radius of the rotating and stationary plates

R_{start} radial position where numerical simulations begin, slightly greater than R_{inlet}

R_{wall} radius of an analogous plug-flow tubular bioreactor

Re Reynolds number, defined by Eqs. (17) and (18)

Sc Schmidt number; ratio of the momentum diffusivity to the mass diffusivity

s_G rate of entropy generation in binary mixtures; dimensions of entropy per volume-time

t independent time variable to describe dynamic behavior of the rotating plate

T absolute temperature

v velocity vector

∇v velocity gradient tensor, and its magnitude $|\nabla v|$

$\{\nabla v\}^T$ transpose of the velocity gradient tensor

v_r radial-component of the local fluid velocity vector, $v_r(r,z)$

v_Θ tangential-component of the local fluid velocity vector, $v_\Theta(r,z)$

$<v_r>_{Average}$ averaged radial-component of the velocity vector, evaluated at $r=R_{Plate}$

z independent spatial variable measured from the stationary to the rotating plate

Δz step size in the axial coordinate measured from the stationary to the rotating plate

Greek symbols

∇ gradient operator

$\beta_{0,nth\text{-}Order}$ stress-free Damköhler number for nutrient consumption by nth-order kinetics

$\beta_{0,Cells}$ stress-free Damköhler number for nutrients consumption by complex cell-based kinetics

β_{Stress} stress-dependent Damköhler number for nutrient consumption by zeroth-order kinetics

$\delta_{Diffusivity}$ nutrient/cell diffusivity ratio

$\varepsilon_{Cell}/\varepsilon_{Nutrient}$ ratio of cell mass produced relative to nutrient mass depleted during nutrient consumption and cell proliferation

$\varepsilon_{Oxygen}/\varepsilon_{Nutrient}$ ratio of oxygen mass depleted relative to nutrient mass depleted during nutrient consumption

ϕ angular displacement of the oscillating upper plate at $z=2B$, given by Eq. (27)

φ dimensionless cell–cell interaction energy in the Fowler–Guggenheim modification of the Sipps isotherm

Γ dimensionless ratio of the magnitude of the velocity gradient tensor, evaluated at radial positions r and at the outer edge of the rotating plate

$\kappa_{Association}$ dimensionless association equilibrium constant for receptor-mediated cell–protein binding

λ exponent in the Sipps isotherm; inverse of the Hill coefficient; $\lambda=1$ for non-cooperative cell–protein binding; $0<\lambda<1$ for positive cooperativity; $\lambda>1$ for negative cooperativity.

μ_i chemical potential of species i

η dimensionless spatial coordinate in the radial direction, $r/2B$

η_{start} initial value of dimensionless radial coordinate for numerical integration

υ_{Heart} frequency of physiological heartbeats, ≈1 cycle/s

Ψ_{Cell} dimensionless mass density of cells on protein-coated surfaces

$\Psi_{Nutrient}$ dimensionless mass density of nutrients in the aqueous medium

$\Psi_{Nutrient,Bulk}$ dimensionless bulk mass density of nutrients in the aqueous medium

Ψ_{Oxygen} dimensionless mass density of dissolved oxygen in the aqueous medium

ρ_{Cell} mass density of cells on protein-coated surfaces; g/cm^2

$\rho_{Nutrient}$ mass density of nutrients in the aqueous medium; g/cm^3

$\rho_{Nutrient,Bulk}(r=R_{inlet})$ bulk velocity-weighted area-averaged inlet mass density of nutrients in the aqueous medium

ρ_{Oxygen} mass density of dissolved oxygen in the aqueous medium; g/cm^3

$\tau_{Residence}$ average residence time for radial flow, $2\pi B(R_{Plate})^2/Q_{Volumetric}\approx 400$ s

$\tau_{ViscousStress}$ molecular momentum flux tensor; also, viscous stress tensor

Θ angular spatial variable in cylindrical coordinates; eliminated via symmetry

Θ_{Cell} fractional coverage by anchorage-dependent cells on protein-coated surfaces

Θ_{Vacant} fraction of sites on protein-coated surfaces that are not occupied by cells

$\omega_{ChemicalRx}$ characteristic time constant for nth-order irreversible chemical reaction

ω_{Heart} angular frequency of physiological heartbeats, $2\pi\upsilon_{Heart}\approx 2\pi$ rad/s

Ω constant angular velocity of the rotating plate that contains bound cells, ≈4 rpm

Ξ cell–cell interaction energy in the Fowler–Guggenheim modification of the Sipps isotherm

χ real separation constant in Eq. (14)

ξ_{A1} Onsager diagonal coefficient (i.e., αT) that couples the affinity (i.e., μ_A/MW_A-μ_B/MW_B) to the rate of nutrient consumption

ξ_{A2} Onsager off-diagonal coefficient (i.e., γT) that couples the magnitude of the velocity gradient tensor to the rate of nutrient consumption

ζ dimensionless independent spatial variable measured in the coordinate direction from the stationary plate to the rotating plate, $z/2B$

Acknowledgements

LA Belfiore gratefully acknowledges the Provincia Autonoma di Trento for supporting his “SmartBone” research project while on sabbatical at the University of Trento, as well as the Polymers Program in NSF's Division of Materials Research via Grant# DMR-0320980. Professor Matt Kipper in the Department of Chemical and Biological Engineering at Colorado State University provided excellent information about receptor-mediated cell–protein binding, the formation of receptor complexes, cell surface diffusion, no-slip boundary conditions that compete with elastic cell response, and rates of nutrient consumption. Dr. Antonella Motta and Professor

Claudio Migliaresi in the Department of Materials Engineering and Industrial Technologies at the University of Trento are acknowledged for insightful discussions about rates of cell proliferation in the presence of mechanical stress, cell–protein docking, and cell–cell attraction on protein-coated surfaces. Finally, Professor Naz Karim in the Department of Chemical Engineering at Texas Tech University provided invaluable data about cell death to justify its exclusion from this manuscript.

References

[1] D.D. Fitts, Nonequilibrium Thermodynamics—A Phenomenological Theory of Irreversible Processes in Fluid Systems, McGraw-Hill, 1962, pp. 34–37.
[2] S.R. de Groot, P. Mazur, Nonequilibrium Thermodynamics, Dover Press, 1984.
[3] L.A. Belfiore, Transport Phenomena for Chemical Reactor Design, Wiley, Hoboken, New Jersey, 2003, pp. 700–702, & Chap. 23.
[4] L.A. Belfiore, Effects of the collision integral, thermal diffusion, and the Prater number on maximum temperature in macroporous catalysts with exothermic chemical reaction in the diffusion-controlled regime, Chemical Engineering Science 62 (3) (2007) 655–665.
[5] L.A. Belfiore, Soret diffusion and nonideal Dufour conduction in macroporous catalysts with exothermic chemical reaction at large intrapellet Damköhler numbers, Canadian Journal of Chemical Engineering 85 (3) (2007) 268–279.
[6] K.D. Andrews, P. Feugier, R.A. Black, J.A. Hunt, Vascular prostheses—performance related to cell-shear responses, Journal of Surgical Research 149 (1) (2007) 39–46.
[7] H.B. Wang, Q.P. Huang, X. Lu, J. Qin, Y.L. Wang, S.X. Cai, The effects of mechanical stress on adhesion and proliferation of vascular smooth muscle cells in vitro, Progress in Biochemistry and Biophysics 28 (1) (2001) 103–107.
[8] M. Yanagisawa, N. Suzuki, N. Mitsui, Y. Koyama, K. Otsuka, N. Shimizu, Effects of compressive force on the differentiation of pluripotent mesenchymal cells, Life Sciences 81 (2007) 405–412.
[9] H. Kawashima, M. Ikegame, J. Shimomura, O. Ishibashi, T. Komori, T. Noda, H. Ozawa, Tensile stress induced osteoblast differentiation and osteogenesis in mouse calvarial suture cultures, Journal of Gravitational Physiology 7 (2) (2000) 121–122.
[10] R Sipps; Journal of Chemical Physics, 16, 1948, 490: 18, 1950, 1024.
[11] R.H. Fowler, E.A. Guggenheim, Statistical Thermodynamics, Cambridge University Press, New York, 1939.
[12] R. Roque-Malherbe, Complementary approach to the volume filling theory of adsorption in zeolites, Microporous and Mesoporous Materials 41 (2000) 227–240.
[13] R Palovuori; PhD thesis, Regulation of cell–cell adhesion and actin cytoskeleton in non-transformed and transformed epithelial cells; University of Oulu, Finland (2003), pp. 26–33.
[14] A.V. Hill, The possible effects of the aggregation of the molecules of hemoglobin on its dissociation curves, Journal of Physiology (London) 40 (1910);
A.L. Lehninger, D.L. Nelson, M.M. Cox, Lehninger Principles of Biochemistry, 4th edition, WH Freeman, 2004 Chap. 5.
[15] D. Axelrod, M.D. Wang, Reduction-of-dimensionality kinetics at reaction-limited cell surface receptors, Biophysical Journal 66 (1994) 588–600.
[16] L.A. Olivier, G.A. Truskey, A numerical analysis of forces exerted by laminar flow on spreading cells in a parallel-plate flow-chamber assay, Biotechnology & Bioengineering 42 (8) (1993) 963–973.
[17] H.G. Othmer, S.R. Dunbar, W. Alt, Models of dispersal in biological systems, Journal of Mathematical Biology 26 (1988) 263–298.
[18] R.B. Bird, W.E. Stewart, E.N. Lightfoot, Transport Phenomena, 2nd Edition, Wiley, Hoboken, New Jersey, 2002.
[19] H. Lu, L.Y. Koo, W.M. Wang, D.A. Lauffenburger, L.G. Griffith, K.F. Jensen, Microfluidic shear devices for quantitative analysis of cell adhesion, Analytical Chemistry 76 (2004) 5257–5264.
[20] P. Yu, T.S. Lee, Y. Zeng, H.T. Low, Effect of vortex breakdown on mass transfer in cell-culture bioreactors, Modern Physics Letters B 19 (28–29) (2005) 1543–1546.
[21] W. Zhang, A. Edwards, Mathematical model of nitric oxide convection and diffusion in a renal medullary vas rectum, Journal of Mathematical Biology 53 (2006) 385–420.
[22] L.A. Belfiore, M.N. Karim, C.J. Belfiore, Tubular bioreactor models that include Onsager–Curie scalar cross-phenomena to describe stress-dependent rates of cell proliferation, Biophysical Chemistry 135 (2008) 41–50.
[23] E.A. Botchwey, S.R. Pollack, S. El-Amin, E.M. Levine, R.S. Tuan, C.T. Laurencin, Human osteoblast-like cells in three-dimensional culture with fluid flow, Biorheology 40 (1–3) (2003) 299–306.
[24] A.I. Barakat, A model for shear-stress-induced deformation of a flow sensor on the surface of vascular endothelial cells, Journal of Theoretical Biology 210 (2001) 221–236.
[25] A. Stefanovska, D.G. Luchinsky, P.V.E. McClintock, Modelling couplings among the oscillators of the cardiovascular system, Physiological Measurements 22 (2001) 551–564.
[26] A. Stefanovska, M. Bracic, Reconstructing cardiovascular dynamics, Control Engineering Practice 7 (1999) 161–172.
[27] M.J. Jaasma, F.J. O, Brien, Mechanical stimulation of osteoblasts using steady and dynamic fluid flow, Tissue Engineering: Part A 14 (7) (2008) 1213–1223.
[28] P.M. Doran, Bioprocess Engineering, Academic Press, 1995, p. 276.
[29] S.J. Pirt, Principles of Microbe and Cell Cultivation, Blackwell Scientific, Oxford University Press, 1975.